

Food & Function

Accepted Manuscript



This is an *Accepted Manuscript*, which has been through the Royal Society of Chemistry peer review process and has been accepted for publication.

Accepted Manuscripts are published online shortly after acceptance, before technical editing, formatting and proof reading. Using this free service, authors can make their results available to the community, in citable form, before we publish the edited article. We will replace this *Accepted Manuscript* with the edited and formatted *Advance Article* as soon as it is available.

You can find more information about *Accepted Manuscripts* in the [Information for Authors](#).

Please note that technical editing may introduce minor changes to the text and/or graphics, which may alter content. The journal's standard [Terms & Conditions](#) and the [Ethical guidelines](#) still apply. In no event shall the Royal Society of Chemistry be held responsible for any errors or omissions in this *Accepted Manuscript* or any consequences arising from the use of any information it contains.

1 **New knowledge on the antiglycoxidative mechanism of chlorogenic acid**

2 Beatriz Fernandez-Gomez^a, Monica Ullate^a, Gianluca Picariello^b, Pasquale Ferranti^{b,c}, Maria
3 Dolores Mesa^d, Maria Dolores del Castillo ^{a*}.

4 ^aDepartment of Food Analysis and Bioactivity, Institute of Food Science Research (CIAL,
5 CSIC-UAM), Nicolas Cabrera 9, 28049 Madrid, Spain.

6 ^bIstituto di Scienze dell'Alimentazione (ISA), CNR, Via Roma 52, 83100 Avellino, Italy.

7 ^cDepartment of Agriculture, University of Naples "Federico II", Parco Gussone, Portici (NA)
8 80055, Italy.

9 ^dInstitute of Nutrition and Food Technology "José Mataix", University of Granada, Avenida del
10 Conocimiento s/n Armilla, 18100 Granada, Spain.

11

12 *Corresponding author: Maria Dolores del Castillo, Department of Food Analysis and
13 Bioactivity, Institute of Food Science Research (CIAL, CSIC-UAM), Nicolas Cabrera, 28049
14 Madrid, Spain.

15 Phone: +34 910017953

16 E-mail address: mdolores.delcastillo@csic.es

17

18 **Key words:** Advanced glycation end products (AGEs), chlorogenic acid, methylglyoxal,
19 glycoxidation reaction, antiglycoxidative effect.

20

21

22 **Abbreviations:** AGEs (advanced glycation end products), MGO (methylglyoxal), GO
23 (glyoxal), HCA (hydroxycinnamic acids), BSA (bovine serum albumin), CML (*N*^ε-
24 (carboxymethyl)lysine), CEL (*N*^ε-(carboxyethyl)lysine), AG (aminoguanidine), 5-CQA (5-*O*-
25 caffeoylquinic acid), 3-CQA (3-*O*-caffeoylquinic acid), CGA (3-*O*-caffeoylquinic acid)
26

27

28

29

30

31

32 **Abstract**

33 The role of chlorogenic acid (CGA) on the formation of advanced glycation end-products
34 (AGEs) (glycooxidation reaction) was studied Model systems composed of bovine serum
35 albumin (BSA) (1 mg mL^{-1}) and methylglyoxal (5 mM) under mimicked physiological
36 conditions (pH 7.4, 37 °C) were used to evaluate the antiglycooxidative effect of CGA (10 mM).
37 The stability of CGA under reaction conditions was assayed by HPLC and MALDI-TOF MS.
38 The glycooxidation reaction was estimated by analysis of free amino groups by OPA assay,
39 spectral analysis of fluorescent AGEs and total AGEs by ELISA, and colour formation by
40 absorbance at 420 nm. Structural changes in protein were evaluated by analysis of phenol-
41 bound to protein backbone using the Folin reaction, UV-Vis spectral analysis and MALDI-
42 TOF-MS, while changes in protein function were measured by determining antioxidant capacity
43 using the ABTS radical cation decolourisation assay. CGA was isomerised and oxidised under
44 our experimental conditions. Evidence of binding between BSA and multiple CGA and/or its
45 derivatives molecules (isomers and oxidation products) was found. CGA inhibited ($p < 0.05$) the
46 formation of fluorescents and total AGEs at 72 h of reaction by 91.2 and 69.7%, respectively.
47 The binding of phenols to BSA significantly increased ($p < 0.001$) its antioxidant capacity. A
48 correlation was found between free amino group content, phenol-bound to protein and
49 antioxidant capacity. Results indicate that CGA simultaneously inhibits the formation of
50 potentially harmful compounds (AGEs) and promotes the generation of neoantioxidant
51 structures.

52

53

54

55

56

57 1. Introduction

58 Protein glycation includes an initial formation of Schiff's base, followed by intermolecular
59 rearrangement and conversion into Amadori products. They undergo further processing to form a
60 heterogeneous group of protein-bound moieties, such as cross-linking fluorescent (*e.g.*,
61 pentosidine) and non-fluorescent adducts (*e.g.*, *N*^ε-(carboxymethyl)lysine) (CML), *N*^ε-
62 (carboxyethyl)lysine (CEL)) called advanced glycation end products (AGEs).¹ Pathways of AGE
63 formation involve glucose autoxidation through the generation of α -oxoaldehydes, such as
64 methylglyoxal (MGO), 3-deoxyglucosone and glyoxal. MGO is a major precursor of AGEs,
65 especially CEL, which is capable of binding and modifying a number of proteins (glycoxidation
66 reaction), including bovine serum albumin (BSA), RNase A, collagen, lysozyme and lens
67 crystallins.^{2,3} Protein glycation is known to be involved in the pathogenesis of several age-related
68 disorders like diabetes, atherosclerosis, end-stage renal and neurodegenerative diseases.⁴

69 Inhibitors of AGEs formation might follow several mechanisms, such as aldose reductase,
70 antioxidant activity, reactive dicarbonyl trapping, sugar autoxidation inhibition and amino group
71 binding.⁵ The inhibition of AGE formation by synthetic aminoguanidine (AG) has been widely
72 documented. However, as AG treatment in type 1 diabetics has caused serious complications,
73 the search for natural AGE inhibitors is currently a challenge.⁶

74 Coffee and yerba mate are considered natural sources of abundant phenolic compounds that can
75 inhibit the formation of AGEs.^{7,8} The most representative phenolic acids in these foods are
76 chlorogenic acids (CGA), which commonly occur as 5-*O*-caffeoylquinic acid (5-CQA) or 3-*O*-
77 caffeoylquinic acid (3-CQA).^{9,10} The antiglycation activity of CGA has been associated to its
78 antioxidant and chelating characters, as well as to its ability to trap reactive dicarbonyl
79 compounds.^{8,11} This study aimed to obtain a better understanding of the antiglycoxidative
80 mechanism of action of CGA which is partly unknown. *In vitro* studies mimicking
81 physiological conditions were performed to achieve this goal.

82 2. Materials and methods

83 2.1 Materials

84 All chemicals and solvents were of analytical grade. Bovine serum albumin (BSA), phosphate
85 buffered saline (PBS), 3-*O*-caffeoylquinic acid (CGA), sodium azide, *ortho*-phthalaldehyde
86 (OPA), *N*^α-acetyl-L-lysine, Folin-Ciocalteu, 3,3', 5,5'-Tetramethylbenzidine (TMB) were from
87 Sigma–Aldrich (St. Louis, USA). Other chemicals and their suppliers were as follows: β-
88 mercaptoethanol (Merck, Hohenbrunn, Germany), methylglyoxal solution (MGO) and 2,2'-
89 azino-bis (3-ethylbenzothiazoline-6-sulphonic acid) diammonium salt (ABTS) (Fluka, Buchs,
90 Switzerland) and Bradford reagent for protein assay (Bio-Rad, München, Germany). The
91 Amicon[®] Ultra- 0.5 ml centrifugal filter unit fitted with an Ultracel[®]-30K regenerated cellulose
92 membrane (30 kDa cut-off) was from Merck Millipore Ltd. (Tullagreen, Cork, Ireland).
93 Microtest 96-well plates made from high-quality polystyrene were purchased from Sarstedt AG
94 & Co. (Nümbrecht, Germany). The Costar[®] high binding 96-well EIA/RIA plate was from
95 Corning Incorporated (Corning, NY, USA). The Milli-Q water used in this study was obtained
96 using a purification system (Millipore, Molsheim, France).

97 2.2 Formation of CGA derivatives in control samples

98 2.2.1 HPLC analysis

99 Standard CGA before and after incubation at 37 °C for 24 h were compared to assess the
100 chemical stability of the compound under experimental conditions by reversed phase (RP)
101 HPLC. A modular chromatographer HP 1100 (Agilent Technologies, Palo Alto, CA, USA)
102 equipped with a multi-waves UV-Vis detector was used to analyse samples. The stationary
103 phase was a 250 x 2.1 mm i.d. C18 RP column, particle diameter 4 μm (Jupiter Phenomenex,
104 Torrance, CA, USA). Column temperature was maintained at 37 °C during the HPLC analyses.
105 Separations were carried out at a constant flow rate of 0.2 mL min⁻¹ applying a 5-60% linear
106 gradient of solvent B (acetonitrile/ 0.1% trifluoroacetic acid, TFA) over 60 min, after 5 min of
107 isocratic elution at 5% solvent B. Solvent A was 0.1% TFA in HPLC-grade water. For each run,
108 2.5 μg standard or incubated CGA were diluted 10-fold with 0.1% TFA and injected using a

109 Rheodyne[®] valve. The HPLC separations were monitored at 280, 320 and 360 nm, while UV-
110 Vis spectra (200-600 nm) were recorded using a diode array detector.

111 2.2.2 MALDI-TOF-MS analysis

112 Mass spectra of CGA freshly prepared and incubated at 37 °C for 24 h were acquired on a
113 Voyager DE-Pro spectrometer (PerSeptive BioSystems, Framingham, Massachusetts) equipped
114 with a N₂ laser ($\lambda = 337$ nm) operating in both positive and negative reflector ion modes. The
115 matrix was 2,5-dihydroxybenzoic acid (DHB) 10 mg mL⁻¹ in 50% acetonitrile. In the positive ion
116 mode, the matrix solution also contained 0.1% TFA. Spectra were acquired using Delay
117 Extraction technology at an accelerating voltage of 20 kV, exploring the m/z 150–1200 range.
118 Matrix ion signals were excluded by separately acquiring positive and negative spectra of DHB.
119 The mass range was externally calibrated with a mixture of standard polyphenols (Sigma,
120 Milan, Italy). Spectra were elaborated with Data Explorer 4.0.

121 2.3 *In vitro* glycoxidation of proteins

122 Model systems were composed of BSA at a final concentration of 1 mg mL⁻¹ in 0.01 M PBS
123 buffer (pH 7.4) added with sodium azide (0.05%) and MGO (5 mM). Glycoxidation model
124 systems were prepared in the presence or absence of the inhibitor (CGA 10 mM). Prior to
125 initiation of the glycoxidation reaction by addition of MGO, the pH values of all solutions were
126 measured at 25 °C using an electrode pH-meter (Metler Toledo, Spain) to ensure optimal and
127 equal conditions of reaction in all samples (pH=7.4). The model systems were incubated at 37
128 °C for 192 h with constant stirring, and samples were taken after 24, 72, 96 and 192 h. The
129 glycoxidation reaction was stopped by cooling in an ice bath. All samples were prepared in
130 triplicate. A control solution of BSA was also included. The progress of the glycoxidation
131 reaction was determined by analysing free amino groups, AGEs and brown compounds.

132

133 2.3.1 Free amino groups

134 Free protein amino groups (both N-terminal and epsilon -NH₂ of lysine) were determined by the
135 OPA assay, following Go *et al.*¹² OPA reagent was freshly prepared by dissolving 10 mg of
136 OPA in 250 μ L of 95% (v/v) ethanol and adding 9.8 mL of 0.01 M PBS pH 7.4 and 20 μ L of β -
137 mercaptoethanol. The total volume of reaction was 250 μ L. The reaction was carried out in
138 transparent polystyrene 96-well microtest plate (No. 82.1581). Fluorescence was read after the
139 addition of OPA reagent on a microplate fluorescence reader Biotek SynergyTM HT (Biotek
140 Instruments, Highland Park, Winooski, USA) with excitation at 360 \pm 40 nm and emission at
141 460 \pm 40 nm. Fluorescence was read every 53 s for 15 min. Calibration curves were constructed
142 using standard solutions of *N* ^{α} -acetyl-L-lysine (0.025-1 mM). All measurements were
143 performed in triplicate, and data were expressed as μ g *N* ^{α} -acetyl-L-lysine equivalent per mg of
144 protein.

145

146 2.3.2 AGEs

147 AGE formation was monitored by fluorescence spectrophotometry using a Biotek microplate
148 spectrophotometer at 360 \pm 40 nm and 460 \pm 40 nm as excitation and emission wavelengths,
149 respectively. No dilution was required for the glycoxidation model or the control systems. All
150 measurements were performed in triplicate.

151 The formation of total AGEs-BSA was measured by an indirect ELISA assay in samples
152 incubated for 72 h. A high affinity protein 96-well microplate was coated overnight (4^o C) with
153 100 μ L of protein samples in 0.01 M phosphate buffer (pH 7.4) (5 μ g mL⁻¹). Unbound proteins
154 were washed out with buffer PBS-T (PBS 0.01 M; Tween 0.05%), the wells were blocked with
155 gelatin 0.5% for 1 h at room temperature, then washed out with PBS-T, and the primary
156 antibody (dilution 1:1000) was added for 1 h. A polyclonal rabbit IG antibody which rose
157 against AGEs (AGE 102-0.2, Biologo, Kroshagen, Germany) was used as the primary antibody.
158 After 1 h incubation and five washing steps, the secondary horse radish peroxidase-conjugated
159 mouse anti-rabbit IgG antibody (ABIN376294, antibodies-online Inc., Suite, Atlanta) diluted
160 1:4000 in washing buffer PBS-T was added, incubated for 1 h and washed again. Colour was

161 developed with TMB (100 μ L) and absorbance was read at 650 nm. Values were estimated by
162 comparison with a standard curve of glycated BSA (Methylglyoxal-AGE-BSA, CY-R2062,
163 CircuLexTM, CycLex Co., Ltd, Nagano, Japan). All measurements were performed in triplicate,
164 and results were expressed as μ g of AGEs-BSA per mg of protein.

165 2.3.3 Brown pigments

166 Formation of brown pigments in the samples was estimated by measuring absorbance at 420 nm
167 of the samples at 24, 72, 96 and 192 h, using microplate reader BioTek PowerWaveTM XS.
168 Samples were analysed in triplicate.

169 2.4 Structural changes of proteins

170 Prior to analysis, the protein fraction of samples incubated at 37 °C for 72 h was isolated by
171 ultrafiltration. Samples (0.4 mL) were placed in the sample reservoir of an Amicon[®] Ultra- 0.5
172 mL centrifugal filter unit fitted with an Ultracel[®]-30K regenerated cellulose membrane (30 kDa
173 cut-off) (Millipore Ltd., Ireland) and centrifuged at 14000 g for 40 min at room temperature. The
174 concentrated samples were recovered and diluted in PBS (0.4 mL). Protein concentration was
175 determined by the Bradford micromethod. The isolated protein fraction was used for structural
176 and functional characterisation.

177 2.4.1 UV-Vis spectra

178 A Biotek microplate UV-Vis spectrophotometer equipped with UV KC junior software (Biotek)
179 was used. The spectrum of fractionated samples was measured at 200-790 nm using a quartz 96-
180 well microplate.

181 2.4.2 Total phenolic compounds

182 Total phenolic content (TPC) of the isolated fraction incubated for 72 h was determined using
183 the Folin-Ciocalteu method as described by Singleton *et al.*¹³ adapted to a microplate reader.

184 The reduction reaction was carried out in 210 μL total volume in 96-well microplates (No.
185 82.1581). A 10 μL of sample (appropriately diluted when necessary) was added to 150 μL
186 volume of Folin-Ciocalteu reagent (diluted 1:14, v/v) in Milli-Q water. After exactly 3 minutes,
187 4 mL of 75 g L^{-1} sodium carbonate solution and 6 mL of water were mixed, and 50 μL of this
188 mixture was added to each well. Absorbance at 750 nm was recorded using a microplate reader
189 BioTek PowerWave™ XS. Calibration curves were constructed using standard solutions of
190 CGA (0.1-1 mg L^{-1}), and results were expressed as $\mu\text{g CGA mL}^{-1}$.

191 2.4.3 MALDI-TOF-MS analysis

192 MALDI-TOF mass spectra of samples incubated for 72 h were acquired in the linear positive
193 ion mode using Voyager DE-Pro spectrometer (PerSeptive BioSystems, Framingham,
194 Massachusetts). The accelerating voltage was 25 kV. Sinapinic acid (10 mg L^{-1} in 50%
195 acetonitrile/TFA 0.1%) was used as the matrix. Spectra were externally calibrated using a
196 commercial protein mixture provided by the instrument manufacturer (PerSeptive Biosystems,
197 Framingham, Massachusetts).

198 2.5 Functionality changes in proteins

199 The antioxidant capacity of samples incubated for 72 h was estimated by the $\text{ABTS}^{\bullet+}$
200 decolourisation assay as described by Oki *et al.*¹⁴ 2,2'-azino-bis (3-ethylbenzothiazoline-6-
201 sulfonic) acid radical cations ($\text{ABTS}^{\bullet+}$) were produced by reacting 7 mM ABTS stock solution
202 with 2.45 mM potassium persulfate and allowing the mixture to stand in the dark at room
203 temperature for 12-16 h before use. The $\text{ABTS}^{\bullet+}$ solution (stable for 2 d) was diluted in 5 mM
204 PBS pH 7.4 (1:16 v/v) to an absorbance of 0.70 ± 0.02 at 734 nm. Each sample was dissolved in
205 phosphate buffer (5 mM, pH 7.4) at 0.1 mg L^{-1} . Thirty μL of test sample and 200 μL of diluted
206 $\text{ABTS}^{\bullet+}$ solution were mixed. Absorbance of the samples at 734 nm was measured at 10 min of
207 reaction using BioTek Power Wave™ XS microplate reader. CGA at concentrations of 0.015-
208 0.2 mM was used for calibration.

209 2.6 Statistical analysis

210 Data were expressed as mean \pm standard deviation (SD). Analysis of Variance (more than 2
211 groups), one-way and two-way ANOVA followed by Bonferroni test, were applied to determine
212 differences between means. Differences were considered to be significant at $p < 0.05$.
213 Relationships between the analysed parameters were evaluated by computing Pearson linear
214 correlation coefficients setting the level of significance at $p < 0.001$.

215

216 3. Results

217 3.1 Formation of CGA derivatives

218 Fig. 1a compares the HPLC chromatograms of standard CGA before (lower panel) and after
219 incubation at pH 7.4, 37 °C for 24 h (upper panel). Peaks were assigned based on retention times
220 and UV-Vis spectra. Under our experimental conditions, CGA was converted into two isomers,
221 namely neochlorogenic acid (trans-5-*O*-Caffeoylquinic acid) and cryptochlorogenic acid (4-*O*-
222 Caffeoylquinic acid).

223 The MALDI-TOF-MS (Fig. 1b) demonstrated the co-occurrence of the hydroquinone and
224 quinone forms ($[M + H]^+$ m/z 353 and m/z 355, and $[M + Na]^+$ m/z 375 and m/z 377,
225 respectively) along with the dimeric adducts ($[2M + Na]^+$ m/z 729 and m/z 731), as assigned in
226 the Table 1. No CGA homopolymers were detected by either HPLC or MALDI-TOF-MS.

227

228 3.2 Progress of the glycooxidation reaction

229 The availability of free amino groups was obtained by OPA assay (Fig. 2). Incubation of BSA
230 alone at 37 °C for 192 h did not significantly affect ($p > 0.001$) the availability of free amino
231 groups, indicating the absence of inter-protein cross-linking events. Incubation in the presence
232 of MGO produced a significant decrease ($p < 0.001$) in BSA free amino groups during the
233 incubation period, suggesting that the glycooxidation reaction occurred. Interestingly, the

234 addition of CGA to the glycoxidation mixture (BSA+MGO) also caused a significant decrease
235 ($p < 0.001$) in available free amino groups throughout the whole incubation period. Available
236 free amino groups also decreased when BSA was incubated with CGA alone compared to the
237 protein control and did not significantly differ ($p > 0.001$) from those of the inhibition model
238 composed of BSA, MGO and CGA.

239 Fig. 3 illustrates the formation of fluorescent AGEs during 192 h of glycoxidation reaction. As
240 expected, the protein control (BSA alone) showed very low fluorescence intensity throughout
241 the experiment, due to intrinsic fluorescence caused by the presence of fluorescent amino acids
242 in the protein backbone. The reaction of BSA and MGO produced a significant formation ($p <$
243 0.05) of fluorescent AGEs in a time dependent manner. The presence of CGA efficiently
244 inhibited ($p < 0.05$) fluorescent AGE formation in the glycoxidation model system, while the
245 reaction of BSA and CGA caused a minor formation of fluorescent compounds. Further and
246 more precise information regarding the generation of total AGEs, both fluorescent and non-
247 fluorescence adducts, under our experimental conditions was obtained by indirect ELISA (Table
248 2). The results are consistent with those obtained by fluorescence monitoring. BSA data are
249 considered basal values for all model systems. AGE generation was significantly ($p < 0.05$)
250 inhibited by the presence of CGA in the glycoxidation system.

251 Fig. 4 shows the generation of brown compounds. Absorbance values at 420 nm of mixtures
252 composed of BSA alone and BSA+MGO were very low and not significantly different ($p >$
253 0.05) in any case. The presence of CGA in the model systems induced significant brown
254 compound formation in a time dependent manner. High and similar levels of browning ($p >$
255 0.05) were found in model systems composed of CGA alone and BSA+CGA. The extent of
256 brown compound formation in samples composed of BSA, MGO and CGA was significantly
257 lower ($p < 0.05$) than in the other samples containing CGA.

258 3.3 Structural changes of protein

259 Since significant AGE formation was observed after 72 h of glycoxidation reaction (Fig. 3 and
260 Table 2), those samples were selected for further characterisation. As shown in Fig. 5a, fresh
261 and incubated (37 °C for 72 h) BSA solutions exhibited identical UV-Vis spectra, suggesting
262 that no structural modifications of proteins occurred following heating. Furthermore, the
263 glycoxidation reaction BSA+MGO did not alter the UV-Vis spectrum compared to fresh BSA.
264 In contrast, the protein fraction isolated from the glycoxidation mixture with CGA showed a
265 very different spectrum than that found for the control (BSA) and was very similar to the
266 spectrum of BSA incubated with CGA.

267 Total phenolic content of the samples incubated at pH 7.4, 37 °C for 72 h is shown in Fig. 5b.
268 As expected, significant levels ($p < 0.05$) of phenolic compounds were detected in the protein
269 fractions isolated from the CGA model systems, namely BSA + CGA and BSA + MGO + CGA.

270 MALDI-TOF-MS analysis was performed to confirm the formation of covalent bindings of
271 CGA to the protein backbone at 72 h (Fig. 6). In the spectra corresponding to BSA incubated
272 with MGO, the characteristic peak of BSA was clearly visible with variable mass increases (Fig.
273 6b). Greater mass shifts were observed when BSA was incubated with CGA either in the
274 absence (Fig. 6c) or presence of MGO (Fig. 6d). The mass data suggested that, BSA binds
275 several molecules of CGA and its derivatives in addition to the MGO in these samples, forming
276 a heterogeneous mixture of protein conjugates as reflected by the broadening of BSA peaks
277 (Fig. 6c and 6d).

278 3.4 Changes of protein function

279 The antioxidant capacity of the isolated protein fractions obtained from samples incubated at 37
280 °C for 72 h is shown in Fig. 7. The reaction with MGO did not modify the antioxidant capacity
281 of BSA. The addition of CGA to reaction mixtures caused the formation of compounds (MW >
282 30 kDa) which had antioxidant capacity values of 303.07 and 309.89 $\mu\text{g eq-CGA mL}^{-1}$ for
283 model system composed of BSA+MGO+CGA and BSA+CGA, respectively.

284 3.5. Correlation between parameters

285 A significant negative correlation ($r=-0.754$, $p < 0.001$) between data corresponding to free
286 amino groups and antioxidant capacity was observed for samples incubated at 37 °C for 72h. A
287 significant negative correlation ($r=-0.689$, $p < 0.001$) was also found between free amino groups
288 and total phenolic content.

289 4. Discussion

290 In this work we observed that structural changes in CGA produced *in vitro* under mimicked
291 physiological conditions may contribute to the antiglycoxidative properties of this compound.
292 Isomerisation of CGA (3-*O*-caffeoylquinic acid) was induced at pH 7.4 and 37 °C. The
293 formation of neochlorogenic (trans-5-*O*-caffeoylquinic acid) and cryptochlorogenic (4-*O*-
294 caffeoylquinic acid). This is a special case of transesterification reaction altering the
295 structure of chlorogenic acid is known as acyl migration and its very depending on the
296 pH of the medium.¹⁵⁻¹⁷ CGA derivatives such as oxidation products and isomers might be able
297 to act as substrate or/and precursors of the Maillard and polymerisation reactions.¹⁸ The
298 formation of mono-quinones and dimer quinones was also observed in CGA incubated at pH 7.4
299 and 37 °C for 24 h. This is in agreement with the non-enzymatic oxidation of CGA described by
300 Rawel et al.¹⁹

301 Brown compounds may be formed by the Maillard reaction, oxidation of phenols and phenol
302 polymerisation.¹⁸ Our data suggest that the Maillard and phenol oxidation reactions are the main
303 pathways leading to the formation of brown compounds under our experimental conditions. Both
304 CGA and its derivatives are able to react with BSA via the Maillard reaction. However, further
305 studies are needed to determine the chemical nature of new-formed coloured compounds.

306 The observed decrease in the formation of AGEs in the presence of CGA demonstrates the
307 antiglycative activity of this compound. On the other hand, our results suggest conjugation of
308 CGA or its derivatives to free amino groups. A significant negative correlation between content

309 of free amino groups and phenolic compounds was found. These results are in agreement with
310 Rawel et al.²⁰ who reported a decrease in lysine residues due to the reaction of BSA and CGA at
311 room temperature for 24 h. CGA isomers and quinones can interact with proteins forming non-
312 covalent and covalent bonds through the Maillard Reaction¹⁸. Phenolics bind highly nucleophilic
313 thiol, amine groups and hydrophobic aromatic groups of proteins.²¹ Three potential types of non-
314 covalent interactions between hydroxycinnamic acids and proteins have been proposed:
315 hydrogen, hydrophobic, and ionic binding.²² Prigent et al.²¹ found that oxidised CGA induced
316 covalent modification of α -lactalbumin and lysozyme.

317 Soft ionization MS techniques such as MALDI are useful to evaluate the hydroxycinnamates
318 (HCA) covalently bound to proteins.²⁰ MALDI-TOF-MS data suggest the formation of protein-
319 phenol conjugates, inducing MS increments of 1.7 and 1.3 kDa in samples corresponding to
320 BSA+CGA and BSA+CGA+MGO, respectively. The increase of molecular mass is indicative
321 of covalent binding between CGA and/or its derivatives to the protein structure. Data on
322 MALDI-TOF-MS support the data obtained on free amino groups, phenolic compounds and
323 UV-Vis spectra.

324 The formation of complexes by covalent binding of other reactive phenols such as quercetin to
325 BSA exhibiting antioxidant potential have been previously reported.^{23,24} Quercetin and CGA
326 share a high binding affinity for BSA. The ability of these two compounds to form covalent
327 complexes polyphenol-BSA under physiological conditions has been demonstrated.^{25,26} Our
328 results show that CGA causes the formation of molecules (protein-CGA interaction products)
329 with antioxidant capacity.

330 Gugliucci et al.⁸ previously associated the inhibitory capacity against formation of fluorescent
331 AGEs of *Ilex paraguariensis* extracts to the presence of CGA. The inhibitory capacity of CGA
332 was linked to its antioxidant character, chelating properties to transition metals ions, quenching
333 of carbonyl radical species and AGE crosslinking.²⁷⁻²⁹ Other authors have also shown the ability
334 of CGA to inhibit *in vitro* BSA glycation induced by fructose and glucose and the formation of
335 AGE crosslinking from collagen.¹¹ We have recently reported that MGO is effectively trapped

336 by CGA with an IC_{50} of 0.14 mg mL^{-1} .³⁰ In addition to this mechanism, we propose for the first
337 time a relationship between the high binding capacity of CGA to BSA and its antiglycoxidative
338 mechanism of action. Our results suggest MGO and GCA are competing for reactive protein
339 sites (free amine group). This effect prevents MGO from binding to BSA resulting in an effective
340 decrease in AGE formation.

341 Coffee is the major source of CGA on the worldwide diet. CGA from coffee has shown a high
342 bioavailability in humans.³¹ A previous study was conducted by others to evaluate the effect of
343 coffee consumption on the redox status of LDL.³² The authors concluded that drinking 200 mL (1
344 cup) coffee induces an increase in the resistance of LDL to oxidative modification, probably as
345 a result of the incorporation of coffee's phenolic acids into LDL. Further studies will be
346 necessary to identify the bound forms and the nature of the bonds of phenolic acids to LDL
347 particle. However, their results suggest that CGA and/or its metabolites might interact with
348 physiological proteins resulting in an improvement or protection of their functions *in vivo*. The
349 findings of the authors are in line with those produced by us using simplified model systems.

350 In summary, the interaction of CGA and its derivatives (isomers and quinones) to side-chains of
351 protein amino residues reduces the formation of potentially harmful compounds, also called
352 AGEs, and promotes the generation of antioxidant structures, which may be beneficial for human
353 health.

354

355 **Acknowledgements**

356 This study was funded by the projects: AGL2010-17779 and IT2009-0087. B Fernandez is
357 grateful for a FPI-predoc grant from the Ministry of Economy and Competitiveness (Spain).

358

359 **References**

- 360 1. R. B. Nawale, V.K. Mourya and S. B. Bhise, Non-enzymatic glycation of proteins: a cause
361 for complications in diabetes, *Indian J. Biochem. Bio.*, 2006, **43**, 337-344.
- 362 2. Z. Kender, P. Torzsa, K. V. Grolmusz, A. Patócs, A. Lichthammer, M. Veresné Bálint, K.
363 Rácz and P. Reismann, The role of methylglyoxal metabolism in type-2 diabetes and its
364 complications, *Orv. Hetil*, 2012, **153**, 574-585.
- 365 3. K. V. Tarwadi and V. V. Agte, Effect of micronutrients on methylglyoxal-mediated in vitro
366 glycation of albumin, *Biol. Trace Elem. Res.*, 2011, **143**, 717-725.
- 367 4. N. Ahmed, Advanced glycation endproducts-role in pathology of diabetic complications,
368 *Diabetes Res. Clin. Pr.*, 2005, **67**, 3-21.
- 369 5. I. Bousová, J. Martin, L. Jahodár, J. Dusek, V. Palicka and J. Drsata, Evaluation of
370 in vitro effects of natural substances of plant origin using a model protein glycooxidation. *J*
371 *Pharmaceut. Biomed.*, 2005, **37**, 957-962.
- 372 6. P. J. Thornalley, Use of aminoguanidine (Pimagedine) to prevent the formation of advanced
373 glycation endproducts, *Arch. Biochem. Biophys.*, 2003, **419**, 31-40.
- 374 7. E. Verzelloni, D. Tagliazucchi, D. Del Rio, L. Calani and A. Conte, Antiglycative and
375 antioxidative properties of coffee fractions, *Food Chem.*, 2011, **124**, 1430-1435.
- 376 8. A. Gugliucci, D. H. Markowicz Bastos, J. Schulze and M. Ferreira Souza, Caffeic and
377 chlorogenic acids in *Ilex paraguariensis* extracts are the main inhibitors of AGE generation
378 by methylglyoxal in model proteins, *Fitoterapia*, 2009, **80**, 339-344.
- 379 9. M. N. Clifford, Chlorogenic acids and other cinnamates—nature, occurrence, dietary
380 burden, absorption and metabolism, *J. Agric. Food Chem.*, 2000, **80**, 1033-1043.
- 381 10. S. Meng, J. Cao, Q. Feng, J. Peng and Y. Hu, Roles of chlorogenic acid on regulating
382 glucose and lipids metabolism: a review, *Evid. Based Complement. Alternat. Med.*, 2013,
383 DOI: 10.1155/2013/801457.

- 384 11. J. Kim, I. H. Jeong, C. S. Kim, Y. M. Lee, J. M. Kim and J. S. Kim, Chlorogenic acid
385 inhibits the formation of advanced glycation end products and associated protein cross-
386 linking, *Arch. Pharmacol. Res.*, 2011, **34**, 495-500.
- 387 12. K. Go, R. Garcia and F. J. Villarreal, Fluorescent method for detection of cleaved collagens
388 using *O*-phthalaldehyde (OPA), *J. Biochem. Biophys. Methods*, 2008, **70**, 878-882.
- 389 13. V. L. Singleton, R. Orthofer and R. M. Lamuela-Reventós, Analysis of total phenols and
390 other oxidation substrates and antioxidants by means of Folin-Ciocalteu reagent, *Methods*
391 *Enzymol.*, 1999, **299**, 152-178.
- 392 14. T. Oki, M. Masuda, S. Furuta, Y. Nishiba, N. Terahara and I. Suda, Involvement of
393 anthocyanins and other phenolic compounds in radical-scavenging activity of purple-fleshed
394 sweet potato cultivars, *J. Food Sci.*, 2002, **67**, 1752-1756.
- 395 15. S. Li and C.T. Ho, Stability and transformation of bioactive polyphenolic components of
396 herbs in physiological pH. In *Herbs: Challenges in Chemistry and Biology*, ed. American
397 Chemical Society, 2006, ch. 18, pp. 240-253.
- 398 16. S. Deshpande, R. Jaiswal, M.F. Matei and N. Kuhnert. Investigation of acyl migration in
399 mono- and dicaffeoylquinic acids under aqueous basic, aqueous acidic, and dry roasting
400 conditions, *J. Agric. Food Chem.*, 2014, **37**, 9160-9170.
- 401 17. C. Xie, K. Yu, D. Zhong, T. Yuan, F. Ye, J. A. Jarrell, A. Millar and X. Chen, Investigation
402 of isomeric transformations of chlorogenic acid in buffers and biological matrixes by
403 ultraperformance liquid chromatography coupled with hybrid quadrupole/ion
404 mobility/orthogonal acceleration time-of-flight mass spectrometry. *J. Agric. Food Chem.*,
405 2011, **59**, 11078-11087.
- 406 18. Z. Budryn and D. Rachwal-Rosiak, Interactions of hydroxycinnamic acids with proteins and
407 their technological and nutritional implications, *Food Rev. Int.*, 2013, **29**, 217-230.
- 408 19. H. M. Rawel and S. Rohn, Nature of hydroxycinnamate-protein interactions, *Phytochem.*
409 *Rev.*, 2010, **9**, 93-109.
- 410 20. H. M. Rawel, S. Rohn, H. P. Kruse and J. Kroll, Structural changes induced in bovine serum
411 albumin by covalent attachment of chlorogenic acid, *Food Chem.*, 2002, **78**, 443-455.

- 412 21. S. V. Prigent, A. G. Voragen, A. J. Visser, G. A. van Koningsveld and H. Gruppen, Covalent
413 interactions between proteins and oxidation products of caffeoylquinic acid (chlorogenic
414 acid), *J. Sci. Food Agric.*, 2007, **87**, 2502-2510.
- 415 22. T. Dan , L. Hui-Jun, L. Ping , W. Xiao-Dong and Q. Zheng-Ming, Interaction of bioactive
416 components caffeoylquinic acid derivatives in chinese medicines with bovine serum
417 albumin, *Chem. Pharm. Bull.*, 2008, **56**, 360-365.
- 418 23. R. Sascha, H. M. Rawel and J. Kroll, Antioxidant activity of protein-bound quercetin, *J.*
419 *Agric. Food Chem.*, 2004, **52**, 4725-4729.
- 420 24. X. Y. Dong, H. F. Yao, F. Z. Ren and H. Jing, Characteristics and antioxidant activity of
421 bovine serum albumin and quercetin interaction in different solvent systems, *Spectrosc.*
422 *Spect. Anal.*, 2014, **34**, 162-166.
- 423 25. Y. Ni, X. Zhangb and S. Kokotc, Spectrometric and voltammetric studies of the interaction
424 between quercetin and bovine serum albumin using warfarin as site marker with the aid of
425 chemometrics, *Food Chem.*, 2006, **99**, 191-203.
- 426 26. L. Trnkova, I. Bousova, V. Kubicek and J. Drsata, Binding of naturally occurring
427 hydroxycinnamic acids to bovine serum albumin, *Natural Science*, 2010, **6**, 563-570.
- 428 27. H. Y. Kim and K. Kim, Protein glycation inhibitory and antioxidative activities of some
429 plant extracts in vitro, *J. Agric. Food Chem.*, 2003, **51**, 1586-1591.
- 430 28. S. Sang, X. Shao, N. Bai, C. Y. Lo, C. S. Yang and C. T. Ho, Tea polyphenols
431 (–)epigallocatechin-3-gallate: A new trapping agent of reactive dicarbonyl species, *Chem.*
432 *Res. Toxicol.*, 2007, **20**, 1862-1870.
- 433 29. C. H. Wu and G. C. Yen, Inhibitory effect of naturally occurring flavonoids on the formation
434 of advanced glycation endproducts, *J. Agric. Food Chem.*, 2005, **53**, 3167-3173.
- 435 30. M. Mesías, M. Navarro, N. Martínez-Saez, M. Ullate, M. D. del Castillo, F. J. Morales,
436 Antiglycative and carbonyl trapping properties of the water soluble fraction of coffee
437 silverskin, *Food Res. Int.*, 2014, **62**, 1120-1126.
- 438 31. A. Farah, M. Monteiro, C. M. Donangelo and S. Lafay, Chlorogenic acids from green coffee
439 extract are highly bioavailable in humans, *J. Nutr.*, 2008, **12**, 2309-2315.

440 32. F. Natella, M. Nardini, F. Belevi and C. Scaccini, Coffee drinking induces incorporation of
441 phenolic acids into LDL and increases the resistance of LDL to *ex vivo* oxidation in humans,
442 *Am. J. Clin. Nutr.*, 2007, **86**, 604-609.

443

444

445

446

447

448

449

450

451

452

453

454

455

456

457

458

459

460

461

462

463

464

465

466 **Table 1:** MALDI-TOF MS assignments of CGA derivatives.

<i>m/z</i>	Assignment
353.5	[CGA*+H] ⁺ quinone
355.5	[CGA+H] ⁺
375.3	[CGA+Na] ⁺ quinone
377.5	[CGA+Na] ⁺
393.3	[CGA+K] ⁺
399.3	[CGA+2Na] ⁺
415.3	[CGA+Na+K] ⁺
531.4	DHB (matrix) adducts
547.4	DHB (matrix) adducts
551.4	DHB (matrix) adducts
729.6	[CGA+CGAquinone+Na] ⁺
751.6	[CGA+CGAquinone+2Na] ⁺
775.6	[CGA+CGAquinone+3Na] ⁺

*CGA includes the isomers of chlorogenic acid that are undistinguishable by mass spectrometry.

467

468

469

470

471

472

473

474

475

476

477

478

479

480 **Table 2:** Content of total AGEs in samples corresponding to control (BSA), BSA with MGO
 481 (BSA+MGO), BSA with MGO and CGA (BSA+MGO+CGA) and BSA with CGA
 482 (BSA+CGA) incubated at pH 7.4 and 37 °C for 72 h. Concentrations assayed were BSA
 483 1mg/mL, MGO 5 mM and CGA 10 mM. BSA data are considered as initial values.

484

485

486

487

488

489

490

491

492

493

494

495

496

497

498

499

500

501

502

503

504

505

506

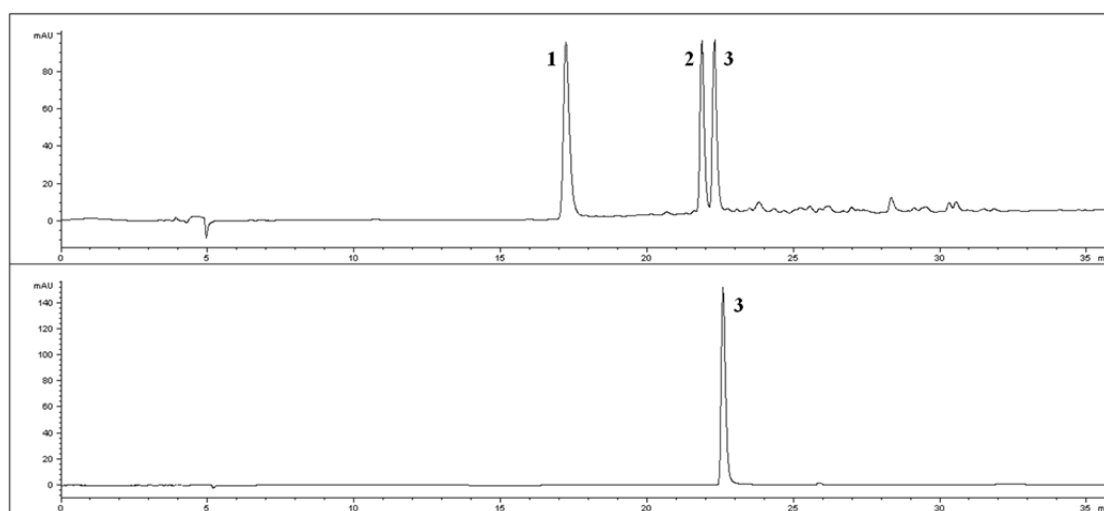
507

Total AGEs ($\mu\text{g AGE-BSA mg}^{-1}$ protein)	Incubation time (h) 72
BSA	1.01 ± 0.08^b
BSA+MGO	1.68 ± 0.13^a
BSA+MGO+CGA	0.51 ± 0.08^c
BSA+CGA	$0.84 \pm 0.19^{b,c}$

Each value represents the mean (n = 9) \pm standard deviation. Different letters denote significant differences ($p < 0.05$) between samples of the same column.

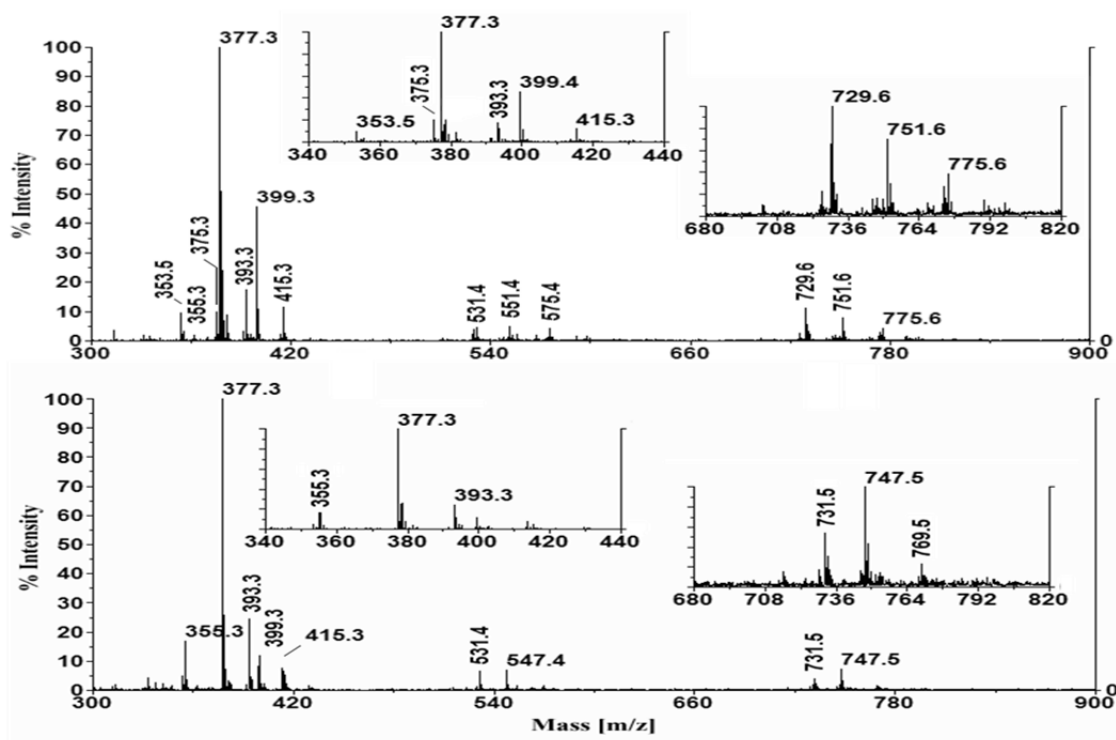
508 **Fig. 1:** (a) RP-HPLC chromatograms of CGA (10 mM) incubated at pH 7.4, 37 °C during 24 h
509 (upper panel) and freshly prepared (lower panel). Peak 1: neochlorogenic acid; Peak 2:
510 cryptochlorogenic acid; Peak 3: chlorogenic acid (b) MALDI-TOF spectra of incubated at pH
511 7.4, 37 °C for 24 h (upper panel) and freshly prepared CGA (lower panel). The spectra have
512 been enlarged (see inserts) to improve the view of relevant ions.

513 **a**



514

515 **b**

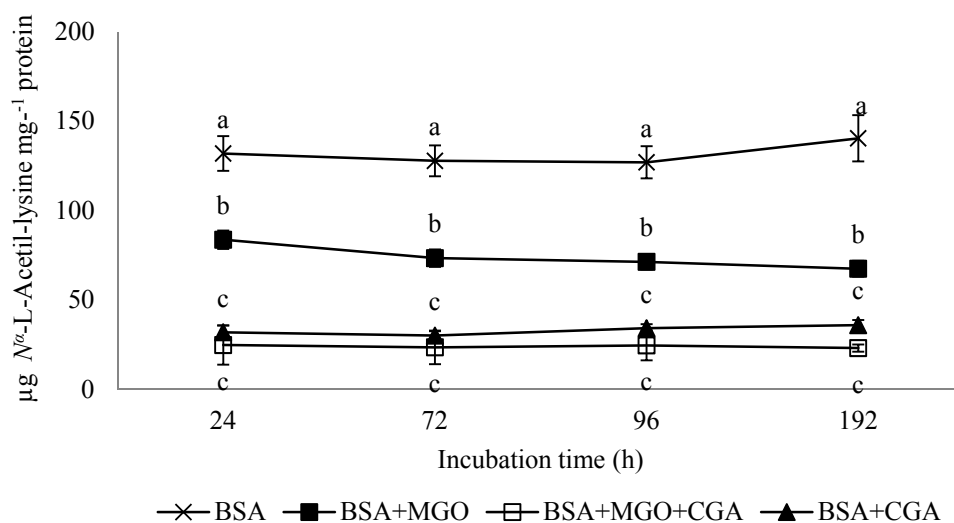


516

517

518

519 **Fig. 2:** Changes in the content of free amino groups in samples of control (BSA), BSA with
 520 MGO (BSA+MGO), BSA with MGO and CGA (BSA+MGO+CGA) and BSA with CGA
 521 (BSA+CGA) incubated at pH 7.4, 37 °C at different times during 192 h. Concentrations assayed
 522 were BSA 1mg/mL, MGO 5 mM and CGA 10 mM. Data are means of triplicate analyses
 523 (n=9). Error bars denote the relative standard deviation. Different letters indicate significant
 524 differences ($p < 0.001$) within model systems at different times. BSA data are considered as
 525 references.



526

527

528

529

530

531

532

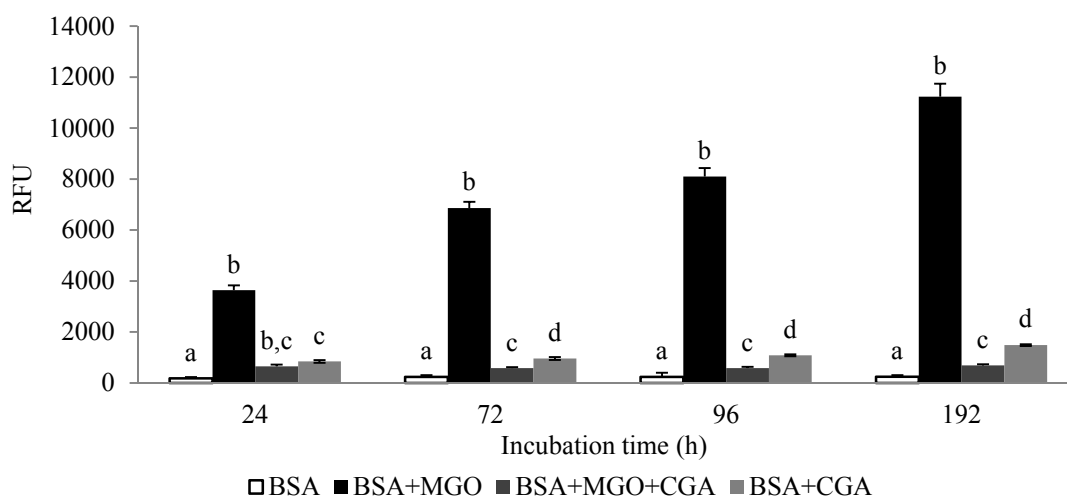
533

534

535

536

537 **Fig. 3:** Time-course of fluorescent AGE formation in samples of control (BSA), BSA with
538 MGO (BSA+MGO), BSA with MGO and CGA (BSA+MGO+CGA) and BSA with CGA
539 (BSA+CGA) incubated at pH 7.4 and 37 °C at different times during 192 h. Concentrations
540 assayed were BSA 1mg/mL, MGO 5 mM and CGA 10 mM. Data represent relative
541 fluorescence units (RFU) (λ_{exc} 360 nm, λ_{em} 440 nm). Bars represent mean values (n=9) and error
542 bars represent standard deviation. Different letters denote significant differences ($p < 0.05$)
543 within model systems at the different times.



544

545

546

547

548

549

550

551

552

553

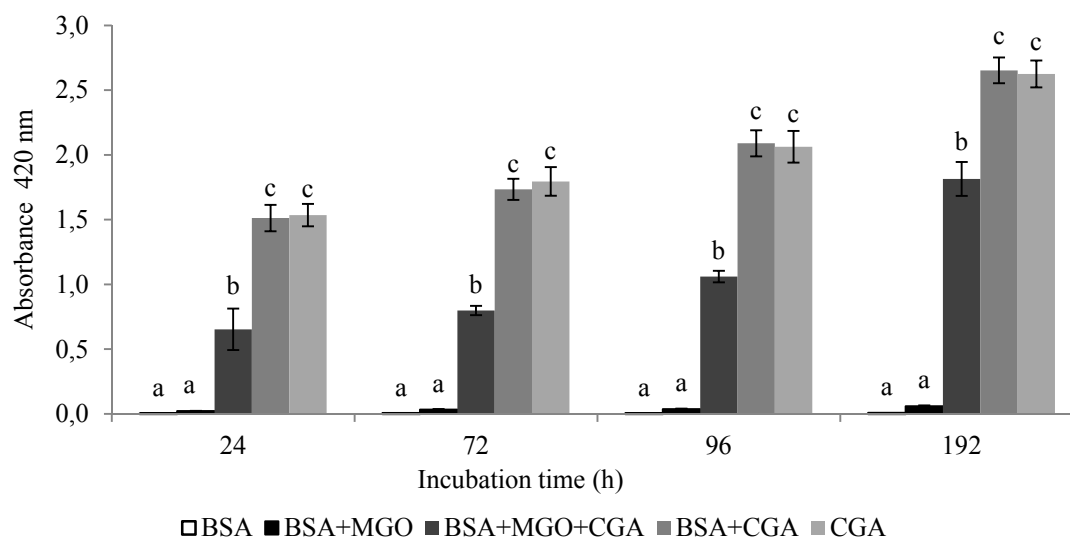
554

555

556

557 **Fig. 4:** Time-course of brown compound formation from control (BSA), BSA with MGO
558 (BSA+MGO), BSA with MGO and CGA (BSA+MGO+CGA), BSA with CGA (BSA+CGA)
559 and CGA control (CGA) incubated at pH 7.4, 37 °C for 192 h. Concentrations assayed were
560 BSA 1mg/mL, MGO 5 mM and CGA 10 mM. Data represent relative absorbance at 420 nm at
561 different time points. Bars represent mean values (n=9) and error bars represent standard
562 deviation. Different letters denote significant differences ($p < 0.05$) within model systems at the
563 different times.

564



565

566

567

568

569

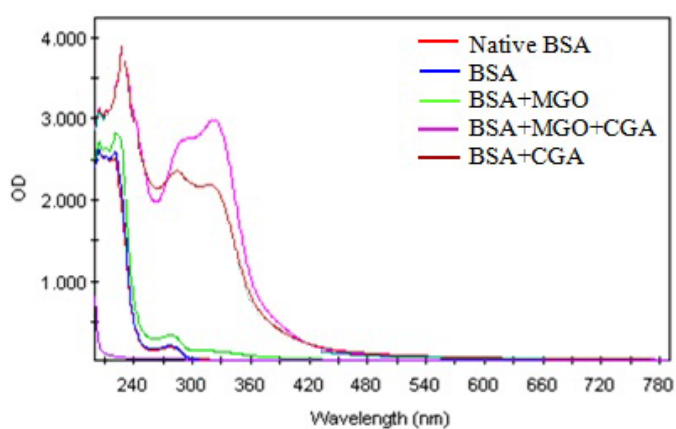
570

571

572

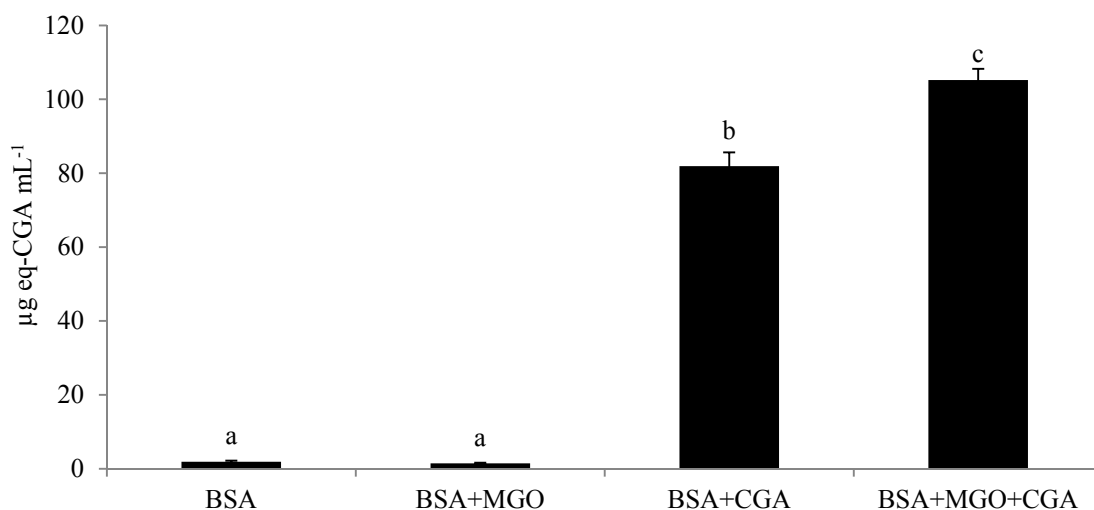
573 **Fig. 5:** (a) UV-Vis absorption spectra and (b) content of phenol compounds bound to BSA
574 isolated from samples corresponding to control (BSA), BSA with MGO (BSA+MGO), BSA
575 with MGO and CGA (BSA+MGO+CGA), BSA with CGA (BSA+CGA) and CGA control
576 (CGA) incubated at pH 7.4 and 37 °C for 72 h. Concentrations assayed were BSA 1mg/mL,
577 MGO 5 mM and CGA 10 mM. Bars represent mean values (n=9) and error bars represent
578 standard deviation. Different letters denote significant differences ($p < 0.001$) between means.

579 **a**



580

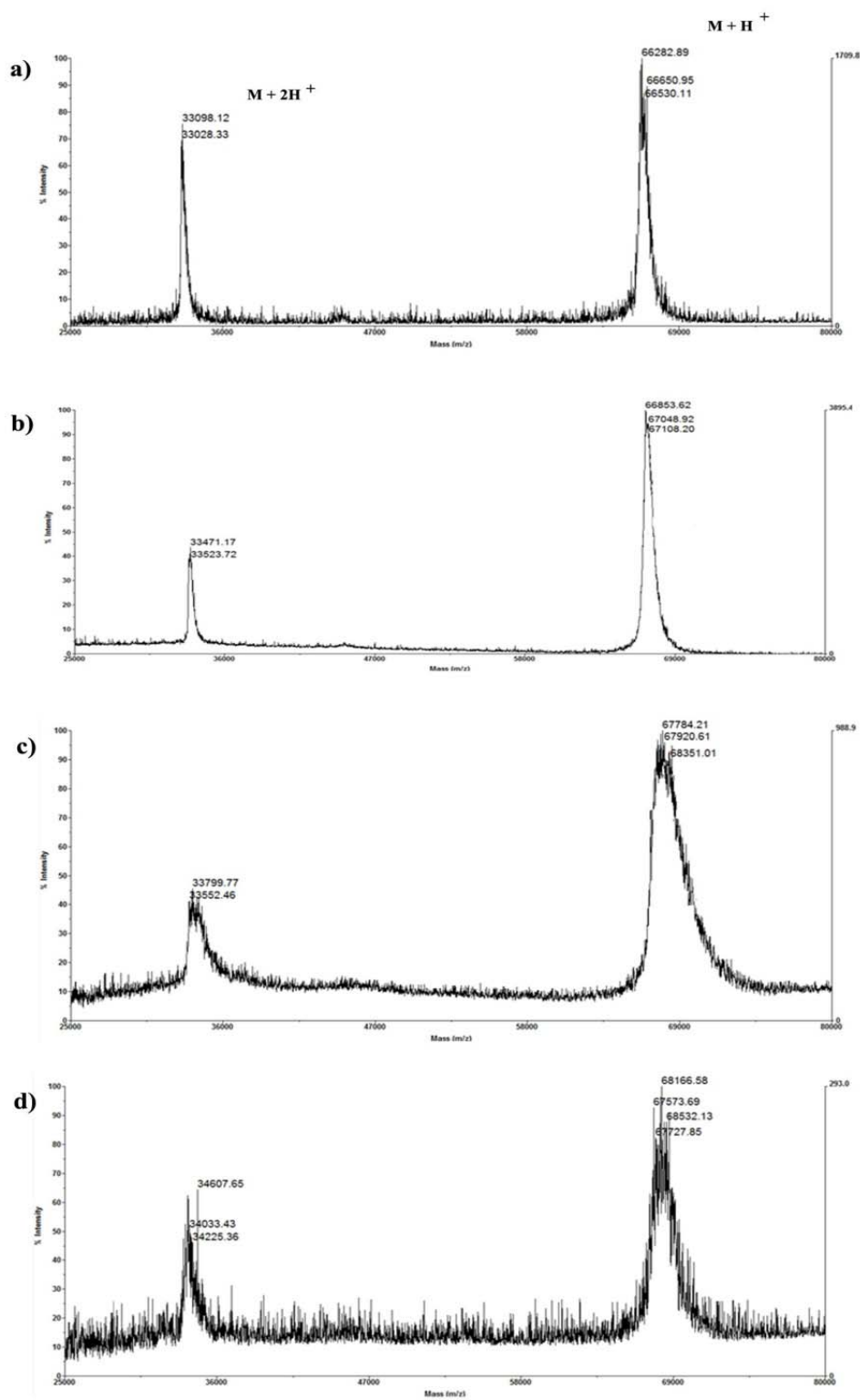
581 **b**



582

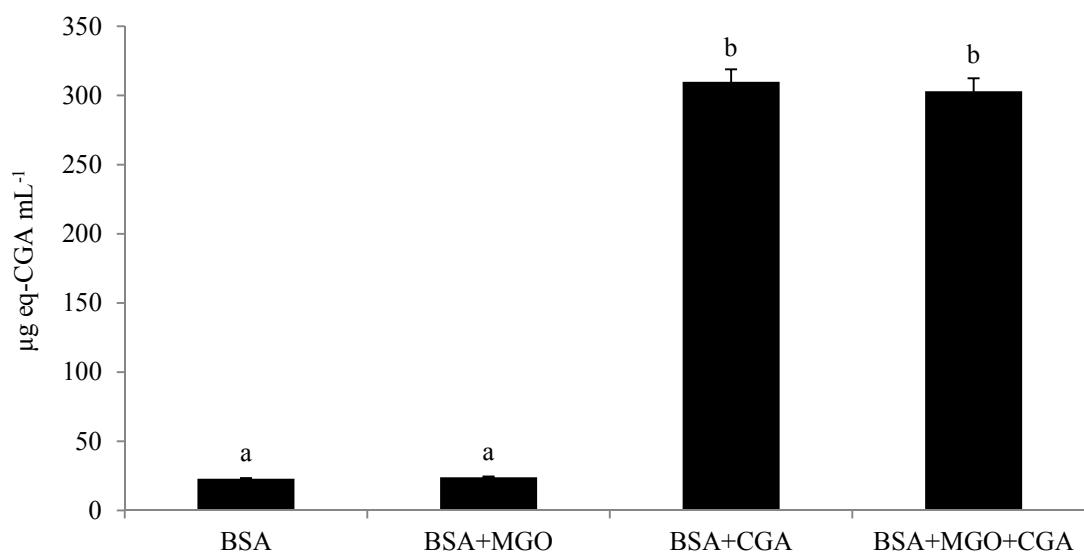
583

584 **Fig. 6:** MALDI-TOF spectra of BSA control (a), BSA with MGO (b), BSA with CGA (c) and
585 BSA with MGO and (d) incubated at pH 7.4 and 37 °C for 72h. Concentrations assayed were
586 BSA 1mg/mL, MGO 5 mM and CGA 10 mM.



587

588 **Fig. 7:** Antioxidant capacity of the high molecular weight fractions isolated from samples of
589 control (BSA), BSA with MGO (BSA+MGO), BSA with MGO and CGA (BSA+MGO+CGA),
590 BSA with CGA (BSA+CGA) and CGA control (CGA) incubated at at pH 7.4 and 37 °C for 72
591 h. Concentrations assayed were BSA 1mg/mL, MGO 5 mM and CGA 10 mM. Data are
592 expressed as $\mu\text{g eq-CGA mL}^{-1}$. Bars represent mean values (n=9) and error bars represent
593 standard deviation. Different letters denote significant differences ($p < 0.001$) between means.



594

595

596

597